geoconvention
Calgary • Canada • June 20-22 2022

Simulated removal of near-surface scattered waves by elastic wave modeling

Ivan J. Sanchez-Galvis[1], William M. Agudelo[2], Daniel A. Sierra[1], Daniel O. Trad[3]
[1]Universidad Industrial de Santander, [2]ECOPETROL S.A., [3]CREWES – University of Calgary

Summary

Ground roll attenuation of seismic data acquired in foothills areas is one of the most challenging problems in land seismic exploration. Irregular topography and near-surface heterogeneities produce near-surface scattered waves that mask the upcoming body-waves reflections. These scattered waves as treated as seismic noise that must be removed in the filtering stage to enhance the reflections. However, conventional methods such as $f-k$ filters don't work properly with this kind of noise because it is in the same frequency-velocity bandwidth than signal and there is not way to know what is the ideal expected result. In this work, we use elastic wave modeling over a 2D profile extracted from the SEAM Foothills model to ideally divide the full wavefield into the near-surface wavefield and deep wavefield. The resulting synthetic data help enhance the understanding of the near-surface scattering behavior and can also be used as a gold standard to design new ground roll filters.

Modeling of near-surface scattering waves

Seismic waves are usually divided into surface waves and body waves. However, In the presence of irregular topography and near-surface heterogeneities, both surface and body waves are scattered producing surface scattered waves and body- scattered waves. All these kinds of waves can be modeled by elastic wave modeling. As equation 1 shows, The full wavefield $\mathbf{u}(\mathbf{x})$ corresponds to the solution of the elastic wave equation in the whole domain and it can be approximated as the sum of surface waves $\mathbf{u}_{SW}(\mathbf{x})$, body waves $\mathbf{u}_{BW}(\mathbf{x})$, surface scattered waves $\mathbf{u}_{SSW}(\mathbf{x})$, and body scattered waves $\mathbf{u}_{BSW}(\mathbf{x})$.

$$\mathbf{u}(\mathbf{x}) \approx \mathbf{u}_{SW}(\mathbf{x}) + \mathbf{u}_{BW}(\mathbf{x}) + \mathbf{u}_{SSW}(\mathbf{x}) + \mathbf{u}_{BSW}(\mathbf{x}) \quad (1)$$

The modeled full wavefield can be divided into Near-surface wavefield and Deep wavefield (equation 2). The Near-surface wavefield corresponds to the solution of the elastic wave equation by using only a portion of the model including only the near-surface part. This Near-surface wavefield includes surface waves and surface scattered waves. Therefore, the Deep wavefield includes body waves and body scattered waves.

$$\underbrace{\mathbf{u}(\mathbf{x})}_{Full\ wavefield} \approx \underbrace{\mathbf{u}_{SW}(\mathbf{x}) + \mathbf{u}_{SSW}(\mathbf{x})}_{Near\text{-}surface\ wavefield} + \underbrace{\mathbf{u}_{BW}(\mathbf{x}) + \mathbf{u}_{BSW}(\mathbf{x})}_{Deep\ wavefield} \quad (2)$$

The Deep wavefield can be computed by subtracting the Near-surface wavefield from the Full wavefield (Equation 3).

$$\underbrace{\mathbf{u}_{BW}(\mathbf{x}) + \mathbf{u}_{BSW}(\mathbf{x})}_{Deep\ wavefield} \approx \underbrace{\mathbf{u}(\mathbf{x})}_{Full\ wavefield} - \underbrace{\mathbf{u}_{SW}(\mathbf{x}) + \mathbf{u}_{SSW}(\mathbf{x})}_{Near\text{-}surface\ wavefield} \quad (3)$$

Numerical example in the SEAM Foothills Phase II model

We perform elastic wave modeling over the SEAM Foothills Phase II to ideally divide the full wavefield into the near-surface and deep wavefield. The SEAM Foothills Phase II is a model designed by the SEG Advanced Modeling (SEAM) Corporation between 2011 and 2016 to understand the complexity of seismic wave propagation in mountainous onshore areas, in particular Andean foothills (Oristaglio, 2013; Regone, 2017). The model covers a region of approximately 14.5 by 12.5 km in horizontal extent and 11 km in depth extent. In our simulations, we use a 2D model section extracted from the SEAM Foothills Phase II along dip line at Y=6.26 km (Figure 1).

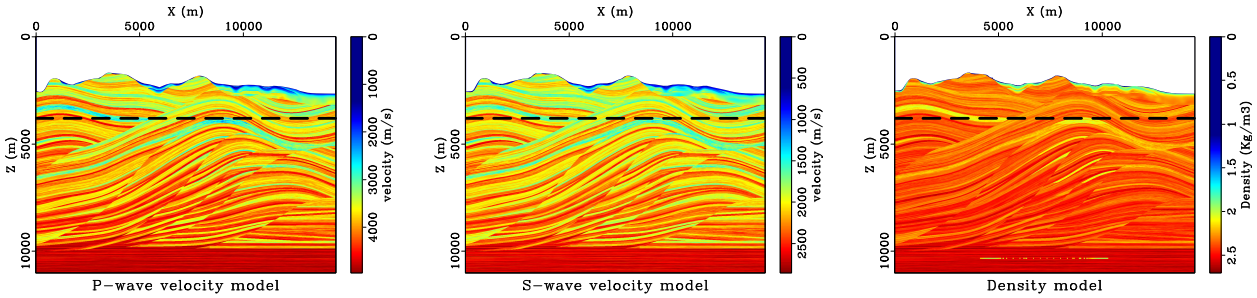

Figure 1. 2D section extracted from the SEAM Foothills Phase II model. The section is a slide along dip line at Y=6.26 km. The dashed line at Z=3800 m indicates the maximum depth of near-surface used in the simulations.

To compute the synthetic data, we use a 2D finite-difference code that uses the parameter-modified method from Cao and Chen (2018) to solve the free-surface condition. We perform the modeling by using a 10 Hz Ricker wavelet source located at X = 5000 m and 10 m depth. The receivers are located at the surface with an interval of 10 m of horizontal distance. We perform 2 simulations to compute the Full and Near-surface wavefield. The first simulation is performed to compute the Full wavefield by using the whole 2D section model in Figure 1. The second experiment is performed to compute the Near-surface wavefield by using only a portion of the 2D section limited by the dashed line along Z=3800 m as shown Figure 1. Finally, the Deep wavefield can be calculated by subtracting the modeled near-surface wavefield from the Full wavefield.

Figure 2 shows three snapshots of the Full, Near-surface, and Deep wavefield of the vertical component velocity. In the snapshots at 5.0 s, it is observed that the Full wavefield and the Near-surface wavefield are equal and there is no Depp wavefield. This is because the Full wavefield is still in the near-surface part above the dashed line. In the snapshots at 1.0 s, the Deep wavefield appears and the Near-surface wavefield is zero below the dashed line. Finally,

in the snapshots at 2.0 s, it is observed that the upcoming body waves from the Deep wavefield are scattered in the near-surface area.

Figure 3 shows the shot gathers from full, near-surface, and deep wavefield of the vertical and horizontal components. Looking at the shot gathers, It seems that Full wavefield and Near-surface wavefield are almost identical. However, it is observed that there is some energy in the Deep wavefield, which is the difference between the Full wavefield and Near-surface wavefield. This result indicates that most of the energy in the Full wavefield corresponds to the Near-surface wavefield and only a minor portion of the Full wavefield corresponds to the Deep wavefield. For this particular example, the Deep wavefield only represents 1.8% of the recorded Full wavefield.

(a) Snapshots at 0.5 s.

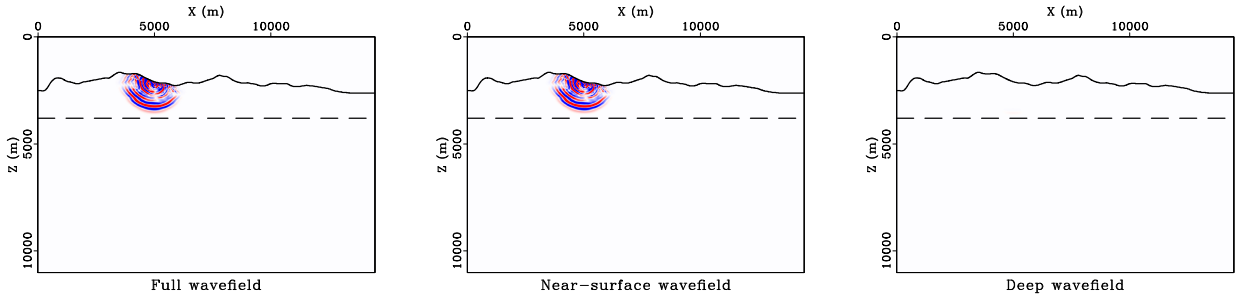

(b) Snapshots at 1.0 s.

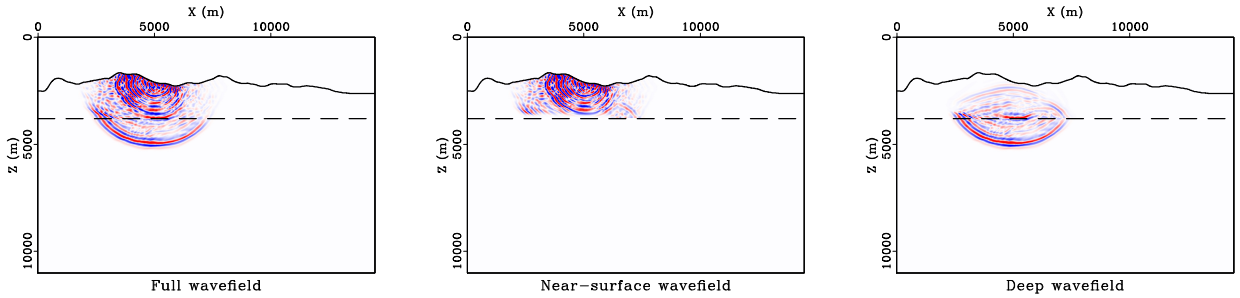

(c) Snapshots at 2.0 s.

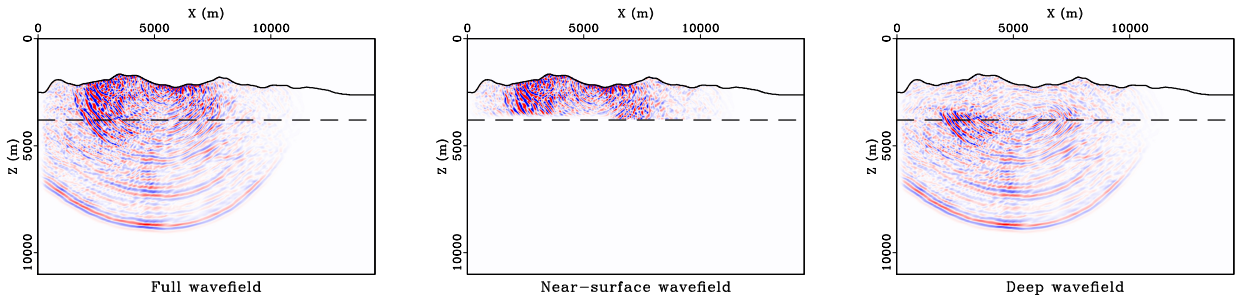

Figure 2. Snapshots of the propagation of full, near-surface and deep wavefield of the vertical component at **(a)**, 0.5 seconds **(b)** 1.0 second, and **(c)** 2.0 seconds.

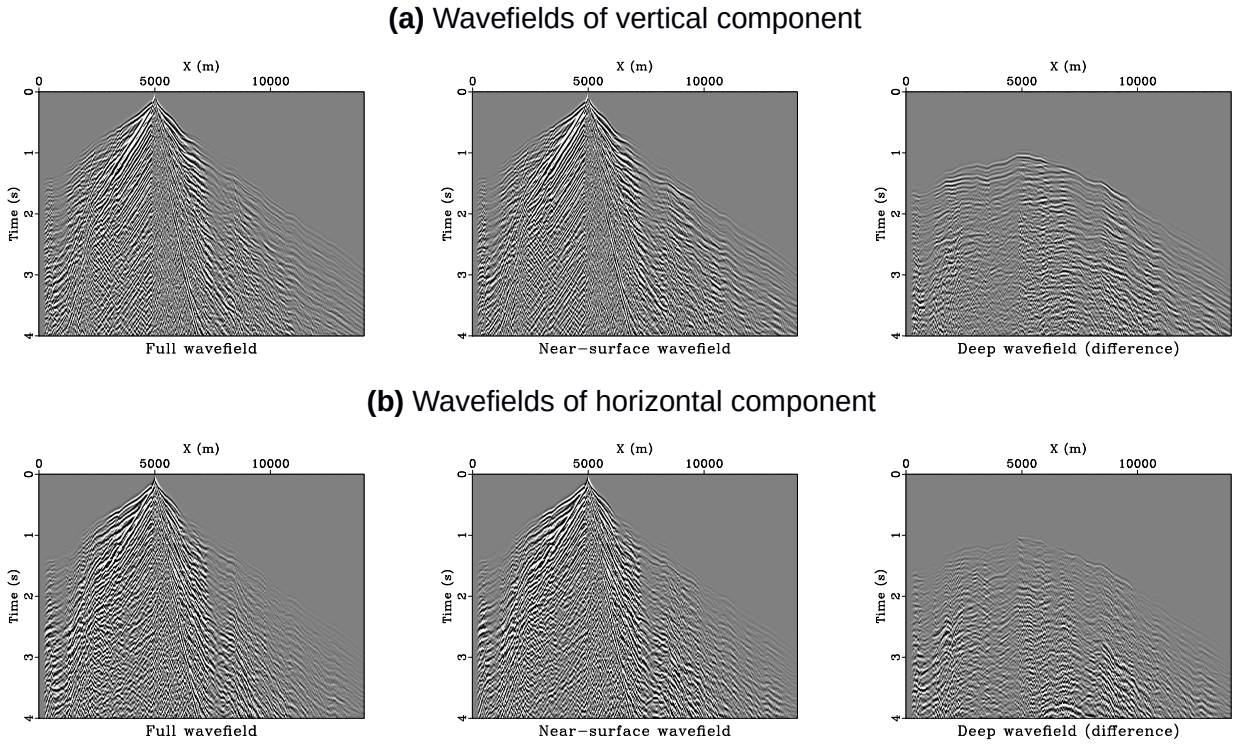

Figure 3. Shot gathers from full, near-surface and deep wavefield of **(a)** vertical component and **(b)** horizontal component.

Discussion and conclusions

Modeling realistic synthetic data requires earth models with the same characteristics as real scenarios. In the case of foothills areas, the earth model must include irregular topography and near-surface heterogeneities to simulate scattered waves. The SEAM Foothills Phase II is a great model to replicate the scattering of surface waves commonly seen in foothills surveys. This model can be even improved by including random near-surface heterogeneities that cause near-surface scattering closer to that observed in real data (Sánchez-Galvis et al, 2021). We used elastic wave modeling over SEAM Foothills Phase II to ideally remove the Near-surface wavefield from the Full wavefield to have a Deep wavefield with the body waves reflections without the ground roll. The computed synthetic data serve as input to understanding near-surface scattering waves besides providing an simulated (“ideal”) expected result for ground roll filter design.

Acknowledgements

This work was carried on the framework of the Agreement “Acta No. 27 del Convenio de Cooperación Tecnológica 5222395” between Universidad Industrial de Santander and Ecopetrol S.A.– Centro de Innovación y Tecnología ICP. The authors also thank to Emerging Leaders in

the Americas Program (ELAP) of Government of Canada for funding a research internship in CREWES-University of Calgary where this work was developed.

References

Cao, J., and J.-B. Chen, 2018, A parameter-modified method for implementing surface topography in elastic-wave finite-difference modeling: Geophysics, 83, no. 6, T313–T332, https://doi.org/10.1190/geo2018-0098.1.

Oristaglio, M., 2013, SEAM update: SEAM Phase II: The Foothills Model — Seismic exploration in mountainous regions: The Leading Edge, 32, no. 9, 1020–1024, https://doi.org/10.1190/tle32091020.1.

Regone, C., J. Stefani, P. Wang, C. Gerea, G. Gonzalez, and M. Oristaglio, 2017, Geologic model building in SEAM Phase II — Land seismic challenges: The Leading Edge, 36, no. 9, 738–749, https://doi.org/10.1190/tle36090738.1.

Sánchez-Galvis, I. J., J. Serrano, D. A. Sierra, and W. Agudelo, 2021. Simulation of scattered seismic surface waves on mountainous onshore areas: Understanding the “ground roll energy cone”: The Leading Edge, 40, no. 8, 601-609. https://doi.org/10.1190/tle40080601.1.